NASA TECHNICAL NOTE

NASA TN D-3741

NASA TN D-3741

A SURVEY OF THERMAL RADIATION STUDIES OF ABLATING BODIES IN THE BALLISTIC RANGE

by William A. Page

Ames Research Center

Moffett Field, Calif.

NATIONAL AERONAUTICS AND SPACE ADMINISTRATION • WASHINGTON, D. C. • FEBRUARY 1967

NASA TN D-3741

A SURVEY OF THERMAL RADIATION STUDIES OF ABLATING BODIES IN THE BALLISTIC RANGE

By William A. Page

Ames Research Center
Moffett Field, Calif.

NATIONAL AERONAUTICS AND SPACE ADMINISTRATION

For sale by the Clearinghouse for Federal Scientific and Technical Information
Springfield, Virginia 22151 – Price $1.00

A SURVEY OF THERMAL RADIATION STUDIES OF ABLATING BODIES IN THE BALLISTIC RANGE*

By William A. Page
Ames Research Center

SUMMARY

Ames Research Center has studied the radiative properties of the boundary layer and near wake of ablating bodies flying in ballistic ranges. The ablating materials investigated include polycarbonate, General Electric 124 resin, polyethylene, polyformaldehyde, Teflon, and cellulose nitrate. Both absolute radiometric and spectrographic data were obtained. The observed absolute amount of radiation varied greatly for the various materials. The chemical species responsible for the radiation in the spectral range from 0.2 to 1.1 μ were CN, C_2, NH, H, and solid carbon microparticles, or soot. The results of the tests indicate a strong correlation between the radiating species present and the carbon-oxygen ratio of the ablating material.

INTRODUCTION

For about ten years, significant research effort has been directed toward the study of thermal radiation emitted by the disturbed flow field about bodies flying at hypervelocities. Two motivations for this research are to study (1) entry body heating resulting from radiative emission and absorption processes in the high-temperature shock layer and boundary-layer gases, and (2) optical signature of missiles during atmosphere entry.

This paper is a survey of some laboratory studies that have been done (refs. 1-4) on this subject and some that are under way in the ballistic ranges at Ames Research Center. Although the studies are somewhat restricted in scope, particularly with respect to the materials investigated, it is useful to gather together the general features of the results and the conclusions that can be made. The laboratory equipment and instrumentation utilized will be described and example results will be shown from studies of the radiative properties of boundary layers on ablating bodies and of the near wake of ablating bodies. Radiation from the high-temperature air in the shock layer (refs. 5-11) will not be discussed. Attention will be directed to the spectral intensity of the radiating sources at model scale and to the measurements and calculations that identify the responsible species.

SYMBOLS

d	model diameter, cm
E	radiation intensity per unit mass of ablated material, W/g
K	wake decay coefficient

*Presented at the Thirteenth National Infrared Information Symposium, Oct. 26-28, 1965, in Pasadena, Calif.

M Mach number

R nose radius, cm

R_λ spectral response of radiometer

T temperature, $^\circ K$

V_∞ free-stream velocity, km/sec

W_λ spectral radiation into 4π steradians, W/μ

x distance downstream from model stagnation point, cm

Δt photographic exposure time, μsec

$\Delta\lambda$ radiometer band pass, μ

λ wavelength, μ

ρ_o sea-level reference density

ρ_∞ free-stream density

APPARATUS, INSTRUMENTATION, AND OPTICAL MEASUREMENT TECHNIQUES

The experimental data described herein have been obtained in several ballistic ranges and/or counterflow ranges (ref. 12) at Ames. Figure 1 shows a typical counterflow range, the pilot hypervelocity free-flight facility. A light-gas gun (ref. 13), utilizing hydrogen as the propellant gas, launches models at hypervelocities into a test section where the velocity and attitude of the model are determined and where radiation measurements can be made. Gun calibers range from 7.1 mm for the pilot facility to 38 mm in the largest Hypervelocity Free-Flight Radiation Facility. The facilities are sufficiently long so that for models made from subliming ablators, the ablation process reaches steady-state conditions, depending somewhat, of course, upon ambient gas density. Velocity up to 9.0 km/sec can be achieved with the guns alone and to 14 km/sec with the shock-tube-driven hypersonic counterflow streams in operation. Most of the results described herein were obtained with a gun alone at typical velocities from 6 to 8 km/sec.

Radiation measurements are made by radiometers that view the test at right angles to the flight path. Figure 1 shows a typical system of narrow-band radiometers, consisting of slits, optical filters, and photomultiplier tubes. Spectral coverage of the radiometers is shown in figure 2 and extends from 0.2 to 1.1 μ, the wavelength range made available by use of photocathode surfaces and fused silica windows. Information has also been collected with image-converter cameras and high-speed-shuttered spectrographs that view the model and wake from the front and from the side.

The radiometers are calibrated in absolute units by reference to a tungsten ribbon filament lamp calibrated by the National Bureau of Standards (ref. 14).

TYPICAL RESULTS

Figures 3, 4, and 5 are image-converter photographs of the luminosity generated by the shock layer, boundary layer, and wake of several models of both blunt and slender shapes made of different ablating materials. These photographs give an idea of the spatial detail of the luminosity about the entry event being simulated in the laboratory. The image-converter camera utilizes an S-11 photocathode; hence, a spectral region from about 0.35 to 0.60 μ is observed. The species responsible for the luminosity recorded in the photographs will be discussed in a later section, Spectrographic Studies.

Figure 6 shows typical results obtained by a spectral radiometer viewing the model flight over a slitted region with a width about as long as the model diameter. The figure shows the variation with time of the spectral radiative intensity from 0.85 to 1.03 μ for two ablating model materials, polycarbonate and polyethylene, and for nonablating aluminum. The initial signal rise represents the arrival of the radiating shock layer into the field of view of the radiometer. For the ablating materials, the additional rise after about $t = 0.7$ μsec is caused by the radiation of the boundary layer flowing along the model sides. The abrupt decay is caused by the radiating shock layer moving out of the field of view. Finally, the second peak and final decay represents radiation from the model wake. Note particularly the effect of model material on the signal. The nonablating aluminum model (which had a relatively cool surface during these observations) shows no wake radiation. The signal is caused by the radiating shock-layer air only, whereas each plastic material adds to this a different intensity level from the boundary layer and near wake for the part of the spectrum being observed.

BOUNDARY-LAYER RADIATION

Now, let us turn our attention to results of observing the radiation intensity of boundary layers on ablating plastic models. Figure 7 presents typical radiometer observations when only the shock layer and forward face of the body are in the field of view. The observed spectral radiation for four plastic materials, polycarbonate, General Electric 124 resin, polyethylene, and polyformaldehyde, is plotted as a function of wavelength. (Cellulose nitrate and Teflon have also been tested with results similar to those for polyformaldehyde.) Observations of a nonablating aluminum model and results from theoretical predictions (ref. 15) for shock-layer air radiance are also shown. Since other test results (ref. 1) utilizing spherical nose models, on the one hand, and flat face models, on the other hand, have demonstrated that little or none of the radiation is emitted by the model surface, the radiation in excess of that from the aluminum model has been attributed to radiation from ablation products, or possible reaction species in the model boundary

layer, or both. This conclusion is consistent with the known low temperature ($< 1000^\circ$ K) of the ablating plastic material. The excess radiation is greatest for polycarbonate, with decreasing amounts observed (in order) from GE 124 resin and polyethylene. The results from polyformaldehyde, cellulose nitrate, and Teflon do not differ appreciably from those for the nonablating model. Note also that the excess radiation from polycarbonate, GE 124 resin, and polyethylene seems to be confined to the visible and infrared portions of the spectrum, with the greatest intensity near 0.7 μ.

It is not immediately obvious from these measurements what boundary-layer species are responsible for the radiation. Clearly, the spectral resolution is insufficient. Much has been learned about the radiation, however, by empirical correlation (ref. 1). It was assumed that the boundary-layer radiative intensity from 0.45 to 1.1 μ could be described by the relation

$$E = k\rho^{\zeta}T^{\xi} , \qquad W/g$$

where E is the radiation per unit mass of ablated material, k is a constant, ρ and T are local values of density and temperature in the boundary layer, and ζ and ξ are exponents which along with k, can be found by correlating the experimental data obtained over a range of free-stream densities and flight velocities. The results obtained by the application of the above equation, along with simple boundary-layer theory for the diffusion process of ablation species in the boundary layer, are shown in table I for three plastic ablating materials. For the blunt-body tests the free-stream density was varied by a factor of 10, while the boundary-layer-edge temperature ranged from 5700° to 8600° K. Insufficient data were collected to establish the value of ξ except for polycarbonate; for the other two materials, a ξ of 4 was assumed. The range of environmental conditions has been substantially increased, however, by a series of tests (ref. 3) in which 30° half-angle-cone models were used. Here the typical boundary-layer-edge temperature was substantially reduced to about 3000° K. The cone results correlate best with the blunt-body results when the values of ξ listed in table I (in the column headed "30° cone tests") are used. It appears from these results that the temperature exponent has been established to well within 25 percent.

TABLE I.- EMPIRICAL CORRELATIONS OF BOUNDARY-LAYER RADIATION;
$E = k\rho^{\zeta}T^{\xi} , \qquad W/g$

Material	k	ζ, Blunt-body tests	ξ, Blunt-body tests	ξ, 30° cone tests
Polycarbonate	7×10^{-8}	0	3.5 ± 1	3.3
GE 124 resin	6×10^{-7}	.66	4(assumed)	---
Polyethylene	2×10^{-8}	.12	4(assumed)	4.3

RADIATION FROM THE NEAR WAKE

More information has been collected about the radiative properties of ablation products by studying the radiation from the near wake. Under most circumstances, there is a peak in wake radiation from 3 to 10 body diameters downstream of the body. Figure 8 presents the values of the peak wake spectral radiation intensity observed (ref. 2) for six model materials flying at a free-stream density ratio of $\rho_\infty/\rho_o = 0.08$ and at velocities (noted along the right side of the figure) of about 6 km/sec. The graph shows almost three orders of magnitude variation in the radiation intensity. Because there could be contributions from scattered light from the relatively much more intense shock layer of the aluminum, polyformaldehyde, and Teflon models, the values plotted for these materials are considered upper limits to the wake radiation. The figure shows that the brightness ranking of the materials, namely, polycarbonate, followed by GE 124 resin, polyethylene, and polyformaldehyde, is the same as that determined for boundary-layer radiation. Hence, a strong relationship exists between radiation from the boundary layer and from the near wake. Note particularly that the infrared radiation from polycarbonate was as intense as was noted for the boundary-layer radiation. Results in reference 2 have established that the peak radiation per unit volume of the near wake varies directly with free-stream density and approximately with the seventh power of the velocity.

The boundary-layer and near-wake radiation is compared further in figures 9 and 10, where the spectral radiation intensity of the boundary layer ($x/d = 0$) is plotted along with the spectral radiation intensity of the wake observed at different distances behind the body. The graphs present results for three plastic materials and for nonablating aluminum, all taken at a free-stream density ratio of $\rho_\infty/\rho_o = 0.08$ and at nearly the same velocity. It is seen that the spectral quality for a given model material changes but little as the ablation products flow from the boundary layer to the wake. Even the apparent change in spectral shape for polyethylene is a result of the data for $x/d = 0$ containing a contribution from shock-layer-air radiation. (The nonablating aluminum data for $x/d = 0$ are a measure of this air radiation.) Hence, if the results for aluminum are subtracted from those for polyethylene, the spectral shape will be almost identical to that of the near wake. There is strong evidence, therefore, that for the conditions of these small-scale tests, the ablation species causing the major portion of the observed radiation do not change (i.e., undergo chemical reaction) as they move downstream from the boundary layer to the wake.

Other properties of wake radiation are of interest; one in particular, is the rate of decay with downstream distance. Measurements (ref. 2) have shown that the decay coefficient K, defined by

$$W_\lambda/W_{\lambda_o} = e^{-Kx}$$

is insensitive to ablation material and the portion of the spectrum under observation, demonstrating a square-root dependence upon free-stream density

only. This behavior was observed for a free-stream Reynolds number range from 40,000 to 600,000, based upon body diameter.

For this Reynolds number range and for body diameters of about 1 cm, the value of K varied from 0.056 to 0.28. Image-converter pictures showed turbulent wakes for these conditions.

SPECTROGRAPHIC STUDIES

Thus far some of the general radiation properties of ablation products in the boundary layer and near wake for a group of representative plastic materials have been described. The radiometer results have not defined the ablation species that cause the radiation, but spectrographic results (ref. 16) have positively identified some of the contributors to the radiation. Because of the difficulty in obtaining sufficient radiative intensity for adequate spectrographic exposures, it was necessary to increase model velocities from near 6 km/sec (where most of the radiometer data were obtained) to 8 km/sec. This higher velocity resulted in one noticeable difference which will be discussed subsequently.

The input slit of an f6.3 Jarrel-Ash spectrograph was optically imaged in the center of the test section along the model flight path. An explosive shutter terminated the exposure about 50 μsec (about 40 model diameters) after the model passed the measurement station. Phototube monitors were used to assure that no extraneous radiation from the gun blast entered the spectrograph.

A typical set of results (ref. 16) for two plastic materials, covering the spectral range from 0.25 to 0.80 μ (with a resolution of about 1 Å) in three exposures, is shown in figure 11. The species are identified and their spectral locations are shown on the figure. The spectral lines reaching completely across the photographic images are Mercury lines used for wavelength calibration. The same species, CN_{violet}, C_2 Swan, NH, and H, are present in the ablation products of polycarbonate and polyethylene, but are of greater intensity with polycarbonate. It should be remarked that neither the CN_{red} system nor, for that matter, any other discernible line or band structure (excepting H_α), is evident in the infrared. Only the faintest evidence of a continuum can be found in the infrared portion of the spectrum in the polycarbonate exposure to correspond to the intense infrared radiation seen by the radiometers. This result is not surprising, since not only are spectrographs insensitive to continuum radiation, but the combination of spectrograph and infrared film being used here is approximately 50 times less sensitive in the infrared than the spectrograph and film combination used in the ultraviolet portion of the spectrum.

A comparison of the spectrograph with the radiometer data shown on figures 9 and 10, along with the spectral response of the individual radiometers (fig. 2), explains some of the bumps in the radiometer records. It is reasonable to assume that the C_2 Swan band system causes increased radiometer output at 0.52 μ in figure 9(a). (The effect of the other strong

$C_{2\ Swan}$ band head, at 0.47 μ, is suppressed by almost a factor of 3 by the relative response of the radiometer centered at 0.455 μ.) The somewhat anomalous result that the output of the radiometer centered at 0.37 μ is not enhanced because of the CN_{violet} band system is explained in part by the effect of increased velocity documented in the radiometric data (ref. 2), but not presented here. The data of reference 2 show substantially increased spectral radiance for the radiometer centered at 0.37 μ when velocity is increased above 6 to 7 km/sec.

We must conclude, therefore, that while the present spectrographic results from the ballistic range identify some of the carbon-bearing ablation species, they provide only faint evidence of a continuum source to account for the most intense feature of the low-resolution radiometer results. Reasonably positive identification of the cause of the infrared radiation, namely, solid carbon microparticles, or soot, has come from both spectrographic results and other observations and calculations described below.

Spectrographic observations (ref. 16) of a diffusion flame burning in air containing the vaporized products driven from samples of polycarbonate and polyethylene (heated in a retort over a hotplate) show intense continuum radiation in the infrared. Furthermore, the flame soots extensively. Interestingly, under a microscope the soot particles (collected by placing a cold glass microscope slide over the flame) showed almost an exact inverse dependence between the number of particles of a given size present and the square of the apparent particle diameter. This rule applied from maximum diameters of 50 μ down to the smallest particles optically observable, ~0.3-μ diameter. Hence, most of the particles collected on the microscope slide are small, but most of the mass collected is in large particles. Electron microscope observations of soot samples collected by the same technique from diffusion flames of other fuels are described in reference 17, where it is stated that the average particle diameters varied from 0.01 to 0.2 μ. No remarks are made about distribution of particle sizes beyond this range. Hence, it is likely, but not certain, that the particle sizes from the present flames differ from those reported in reference 17.

Shadowgraph pictures of polycarbonate and polyethylene models flying in the ballistic range show partially opaque wakes. Shadowgraphs of models which do not seem to radiate in the infrared show clear wakes. Examples of such shadowgraphs are given in figure 12. Since the spark light with which the shadowgraph is obtained has an effective source temperature above 15,000° K, the solid carbon microparticles are believed to cause the opacity in the polyethylene model wake.

Ablation tests of polycarbonate in arc-jet facilities at Ames and other laboratories have shown carbon deposits, "black carbonaceous tendrils and filaments," (ref. 18) downstream of the model.

Calculations were performed to estimate the absolute spectral radiation that might be observed from the model boundary layer due to the presence of solid carbon microparticles. The following assumptions were made: (a) All carbon in the ablating products is in the form of microparticles, with diameters less than the wavelength of peak spectral emission, an assumption

conforming to reported measurements in diffusion flames (ref. 17). (b) The extinction coefficient is given by a simplified expression arising from the work of Siddall and McGrath (ref. 19), where it is shown, contrary to most reported work, that the extinction coefficient for small particles is independent of particle size; the coefficient depends only upon wavelength and material concentration per unit volume of radiating flame. (c) The boundary layer is optically thin. (d) The mole fraction of microparticles is independent of distance from the wall until the sublimation temperature of carbon is reached, at which time the microparticles disappear. (e) Temperature distribution in the boundary layer is linear starting with 1000° K at the wall. (f) The sublimation temperature of carbon depends on pressure and composition (ref. 20). A sublimation temperature of 4000° K was chosen for the conditions of the example calculation, where the shock-layer pressure is 80 atmospheres.

The calculation was made for the boundary layer on a polycarbonate model with a diameter of 0.71 cm, a nose radius equal to 0.51 cm, $\rho_\infty/\rho_o = 0.19$, and $V_\infty = 5.97$ km/sec and the results are compared in figure 13 with test results. Although the calculation is rather crude, it does demonstrate remarkable agreement in intensity to the test results and about the same relative spectral distribution of radiation. It should be remarked that a calculation based upon microparticles larger than the wavelength of emission would lead to spectral intensities somewhat lower than those determined above, but with little change in spectral distribution.

From all the evidence presented above, it is concluded that solid carbon microparticles are an important source of the infrared continuum in the boundary layer and wake of the models. The possibility that carbon particles are present in the wakes of polycarbonate models has also been reported (refs. 21 and 22).

The species that cause observable radiation from the ablation products in both the boundary layer and near wake are summarized in table II along with the formula and element ratios of carbon to hydrogen, and carbon to oxygen of the plastics investigated. (The comparative intensities listed are representative of conditions near 6 km/sec.)

TABLE II.- FORMULA, ELEMENT RATIOS, AND SPECIES OBSERVED FOR ABLATING PLASTICS

Plastic	Formula	Element ratios		Species observed[a]
		C/H	C/O	
Polycarbonate	$C_{16}H_{14}O_3$	1.14	5.3	$Soot_S$, C_{2S}, CN_W, NH, H
GE 124 resin	~$C_{10}H_{13}O_3$	.77	3.3	$Soot_M$, C_{2W}, CN_M
Polyethylene	CH_2	.5	∞	$Soot_W$, C_{2M}, CN_S, H
Polyformaldehyde	CH_2O	.5	1	H
Cellulose nitrate	$C_6H_8O_9N_2$	.75	.67	

[a]Subscripts indicate comparative radiative intensity: S, strong; M, medium; W, weak.

The effect of C/O ratio and its influence on soot formation in the ablation products are readily apparent and somewhat anticipated. (See, e.g., ref. 17, p. 189, where carbon formation in diffusion flames is discussed in great detail.) When sufficient oxygen is present (i.e., polyformaldehyde and cellulose nitrate), soot formation is totally suppressed. The observations of polycarbonate and GE 124 resin show that increasing the C/O ratio allows more carbon to be formed. The results from the polyethylene test imply that a high hydrogen concentration suppresses soot formation. When considering the effect of C/O ratio on the species formed, it is clearly important also to take into account the air species in the boundary layer and wake that are mixed intimately with the ablation species.

A final remark should be made about the value of the temperature exponent, ξ, determined from the empirical study of radiation from the boundary layer (reviewed in an earlier section of this survey). The following argument has ramifications as to the mechanism of formation of carbon microparticles from the ablation material. The temperature dependence of the radiance for material in the boundary layer is nearly 4. The classical Mie theory of absorption and scattering (ref. 23) of radiation by small solid particles predicts nearly a λ^{-1} wavelength dependence of the extinction coefficient for particles smaller than the wavelength and generally an extinction coefficient independent of wavelength for particles larger than the wavelength. Hence, one would expect a T^5 dependence for radiation emitted by small particles and a T^4 dependence for large particles. This result suggests that large particles exist in the boundary layer. There is also a possibility that the ablation process for the high shock-layer pressure and convective heating load conditions of these small scale tests consists principally of the spallation or shearing of particles from the ablating surface (from thermal shock?) which probably break up, vaporize, and char as they move downstream in the boundary layer and wake flow.

The arguments and conclusions in the above paragraph must still be treated as somewhat tentative pending further developments in both experiment and theory.

CONCLUDING REMARKS

Although only a few ablation materials have been studied thus far, it is clear that the radiance of boundary layers and near wakes depends critically upon the chemistry of the ablation material to the extent that the wake does not radiate measurably (as is the case for the present experimental conditions) in the absence of ablation products. With ablation, radiation from the boundary layer and all stations of the wake have similar spectra. Since only simple carbon-bearing species have thus far been observed, there is no evidence that the polymer structure of the ablation material (as contrasted to the atomic element ratios) influences the observed radiation.

The observed radiation indicates that: (a) Materials with a high carbon-oxygen, C/O, ratio radiate substantially more than those with a low C/O ratio. (b) Materials with high C/O ratios exhibit significant amounts of infrared radiation caused by solid carbon microparticles or soot. (c) Other ablation-product radiators identified are CN_{violet}, C_2 Swan, NH, and H.

(d) The temperature dependence of the infrared radiation (which implies that in the boundary layer the carbon microparticles are large compared to the wavelength of peak spectral emission) has ramifications with respect to the ablation process under high shock-layer pressures and high convective heating loads.

Ames Research Center
National Aeronautics and Space Administration
Moffett Field, Calif., Nov. 1, 1966
129-01-08-16-21

REFERENCES

1. Craig, Roger A.; and Davy, William C.: Thermal Radiation From Ablation Products Injected Into a Hypersonic Shock Layer. NASA TN D-1978, 1963.

2. Stephenson, Jack D.: Measurement of Optical Radiation From the Wake of Ablating Blunt Bodies in Flight at Speeds Up to 10 Km Per Second. NASA TN D-2760, 1965.

3. Davy, William C.; Craig, Roger A.; Chapman, Gary T.; and Compton, Dale L.: Ablation-Products Radiation From Cones. AIAA paper 64-71.

4. Stephenson, Jack D.: Radiation From Wakes of Blunt Bodies at Speeds Up to 32,000 Feet Per Second. Paper presented at 13th Meeting Anti-Missile Research Advisory Council (San Diego, Calif.), Apr. 30, May 1 and 2, 1962.

5. Page, William A.; Canning, Thomas N.; Craig, Roger A.; and Stephenson, Jack D.: Measurements of Thermal Radiation of Air From the Stagnation Region of Blunt Bodies Traveling at Velocities Up to 31,000 Feet Per Second. NASA TM X-508, 1961.

6. Canning, Thomas N.; and Page, William A.: Measurements of Radiation From the Flow Fields of Bodies Flying at Speeds Up to 13.4 Kilometers Per Second. Paper presented to the Fluid Mechanics Panel of AGARD (Brussels, Belgium), Apr. 3-6, 1962.

7. Page, William A.; and Arnold, James O.: Shock-Layer Radiation of Blunt Bodies at Reentry Velocities. NASA TR R-193, 1964.

8. Givens, John J.; Canning, Thomas N.; and Bailey, Harry E.: Measurements of Spatial Distribution of Shock-Layer Radiation for Blunt Bodies at Hypersonic Speeds. NASA TM X-852, 1964.

9. Walters, Edward E.: Free-Flight Measurements of Radiative Heating to the Front Face of the Apollo Reentry Capsule as a Function of Angle of Attack. NASA TM X-851, 1964.

10. Compton, Dale L.; and Cooper, David M.: Measurements of Radiative Heating on Sharp Cones. AIAA J., vol. 3, no. 1, Jan. 1965, pp. 107-114.

11. Reis, Victor H.: Oscillator Strengths for the N_2 Second Positive and N_2^+ First Negative Systems From Observations of Shock Layers About Hypersonic Projectiles. J. Quant. Spectr. Radiative Transfer, vol. 4, no. 6, Nov.-Dec. 1964, pp. 783-792.

12. Seiff, Alvin: A Progress Report on the Ames Hypervelocity Free-Flight Facilities and Some of the Current Research Problems Being Studied in Them. AIAA paper 63-162.

13. Curtis, John S.: An Accelerated Reservoir Light-Gas Gun. NASA TN D-1144, 1962.

14. Stair, Ralph; Johnston, Russell G.; and Halbach, E. W.: Standard of Spectral Radiance for the Region of 0.25 to 2.6 Microns. J. Res. Nat. Bur. Stds., Annals Phys. Chem., vol. 64A, no. 4, July-Aug. 1960, pp. 291-296.

15. Meyerott, R. E.; Sokoloff, J.; and Nicholls, R. W.: Absorption Coefficients of Air. LMSD 288052, Lockheed Aircraft Corp., 1959.

16. Borucki, William J.: Spectrographic Observations of Polycarbonate, Polyethylene, and Polyformaldehyde in a Ballistic Range, an Arc Jet, and a Diffusion Flame. AIAA paper 66-132.

17. Gaydon, A. G.; and Wolfhard, H. G.: Flames, Their Structure, Radiation and Temperature. Second rev. ed., Chapman and Hall Ltd., 1960.

18. Wentink, T., Jr.; Isaacson, L.; and Economou, G. J.: Thermal Degradation of the Plastic Zelux (Lexan). RAD-TM-63-51, AVCO Corp., July 31, 1963.

19. Siddall, R. G.; and McGrath, I. A.: The Emissivity of Luminous Flames. Ninth Symposium (International) on Combustion. Academic Press, 1963, pp. 102-110.

20. Hochstim, Adolf R.: Equilibrium Compositions, Thermodynamic and Normal Shock Properties of Air With Additives. Vol. 1, Rep. ZPh-122, General Dynamics/Convair, 1961.

21. Steinberg, M.; Maiden, C. J.; Leak, W. R.; and Hansen, C. F.: Preliminary Studies of the Effects of Ablation Contaminants on Radiation. TR 62-209H, General Motors Corp., Aerospace Operations Dept., Dec. 1962.

22. Sadowski, C. M.; Dionne, J. G. G.; and Trottier, G.: A Study of Shock-Cap Radiation From 1.0 Inch Diameter Hypersonic Spheres, Part 1, Projectile Velocities to 17,000 Feet Per Second. CADDE-TR-491/64, Canadian Armament Research and Development Establishment, Apr. 1964.

23. Krascella, N. L.: The Absorption and Scattering of Radiation by Small Solid Particles. J. Quant. Spectr. Radiative Transfer, vol. 5, no. 1, Jan.-Feb. 1965, pp. 245-251.

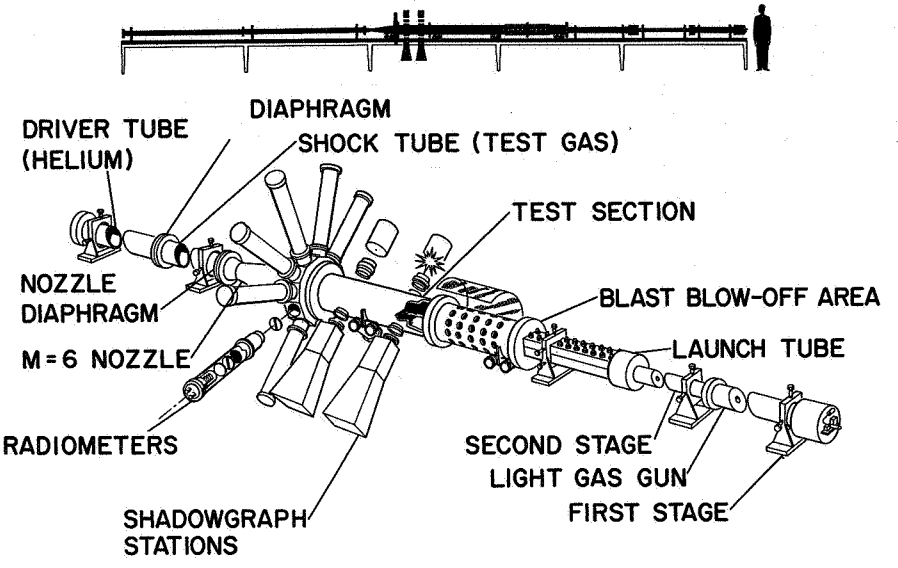

Figure 1.- Schematic drawing of Pilot Hypervelocity Free-Flight Facility.

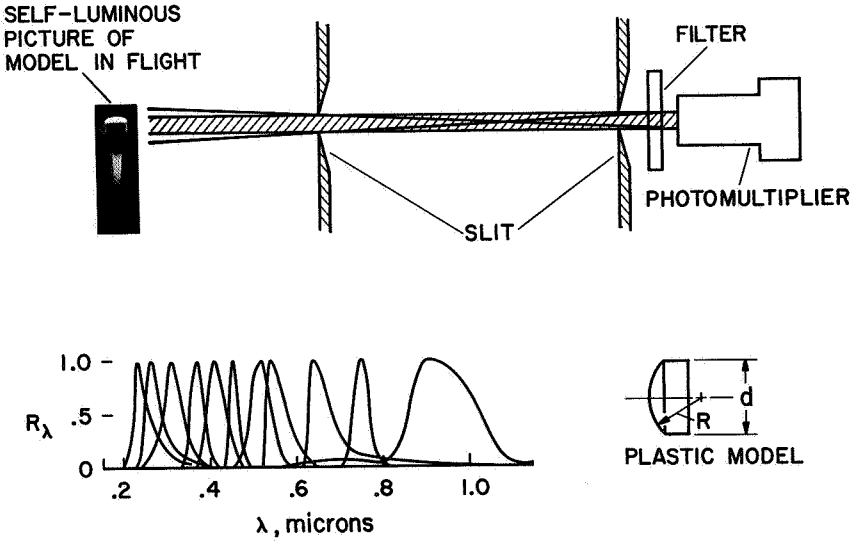

Figure 2.- Sketch of radiometer field of view and responsivities.

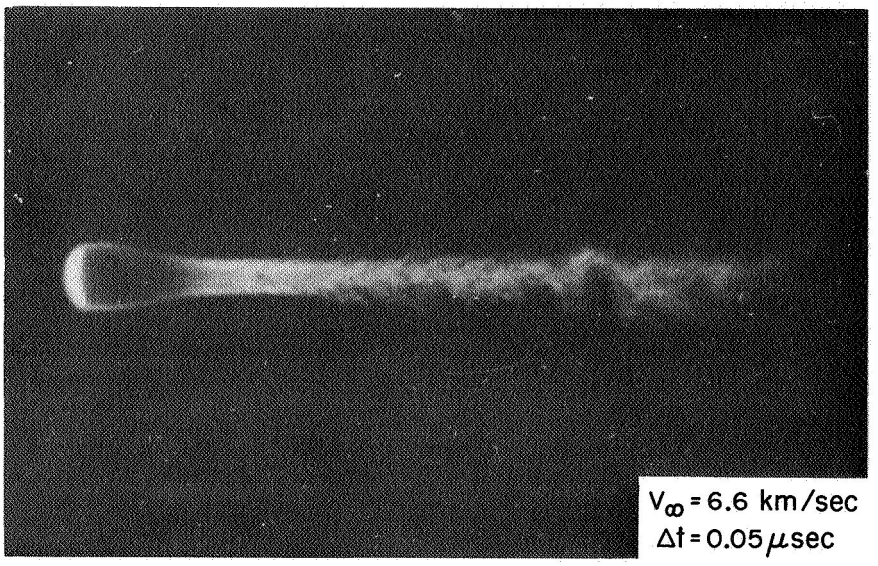

Figure 3.- Self-luminous photograph of ablating polycarbonate model.

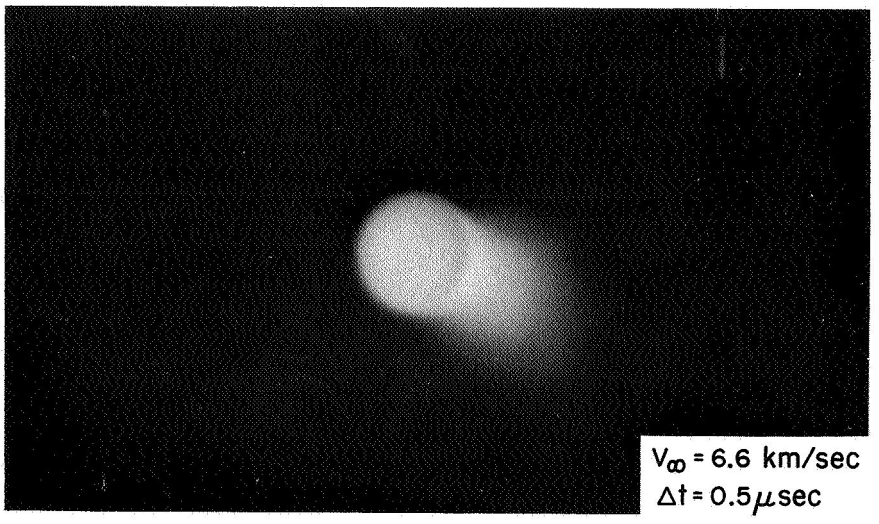

Figure 4.- Self-luminous photograph of ablating polycarbonate model; head-on view.

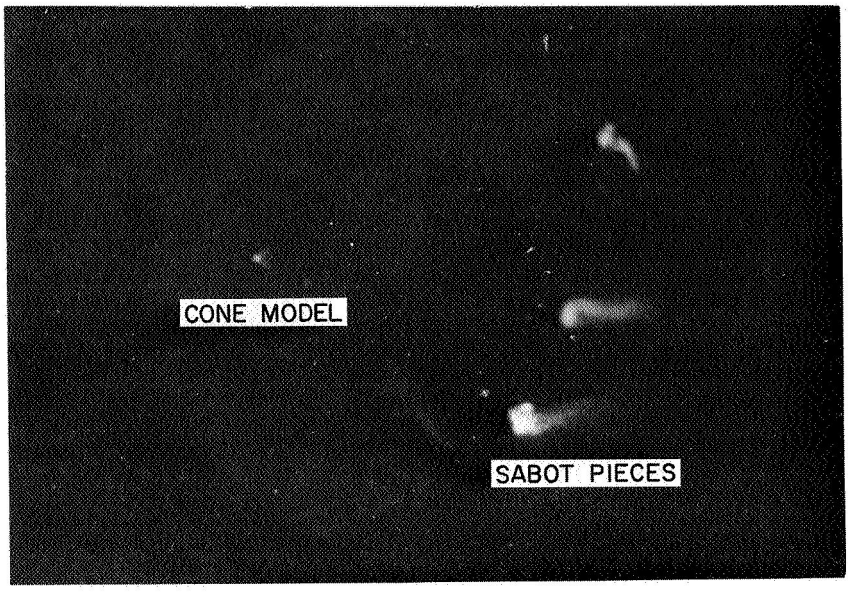

Figure 5.- Self-luminous photograph of ablating Teflon round-nosed cone; V_∞ = 5.9 km/sec, Δt = 0.5 μsec.

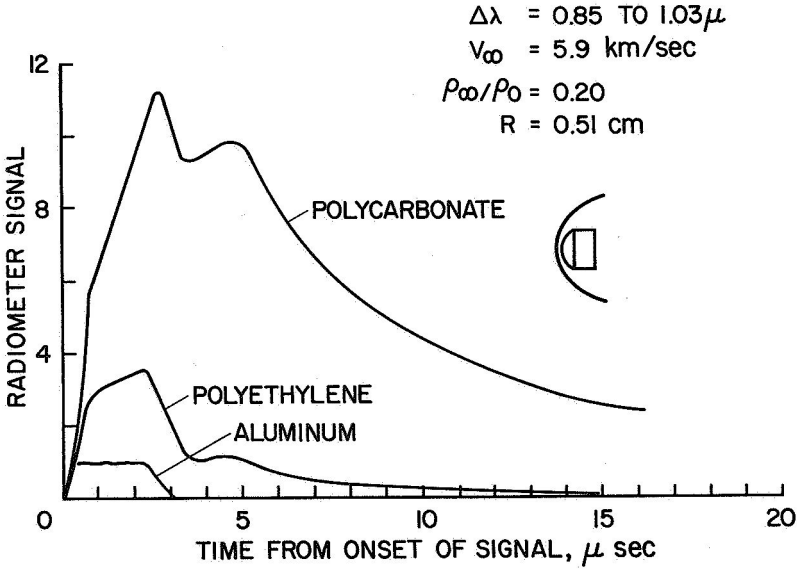

Figure 6.- Variation of infrared radiation with model material.

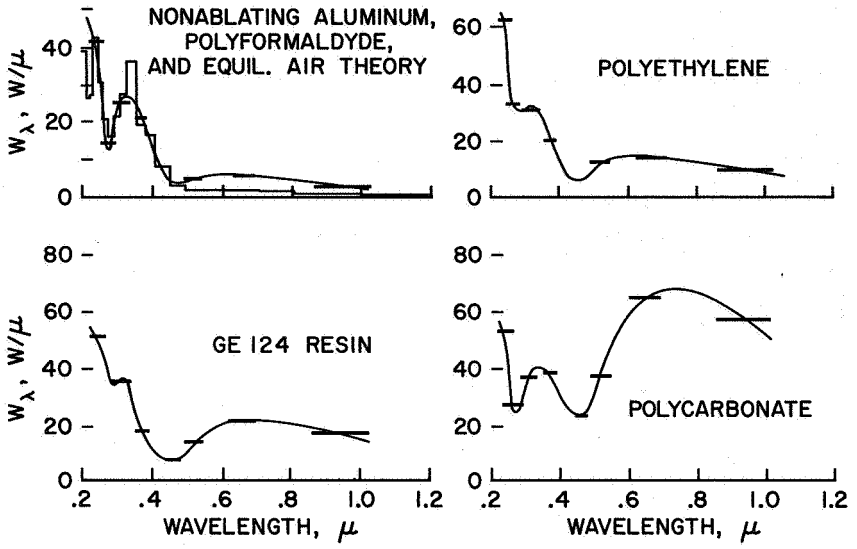

Figure 7.- Radiometric data; $\rho_\infty/\rho_o = 0.08$, $V_\infty = 6$ km/sec.

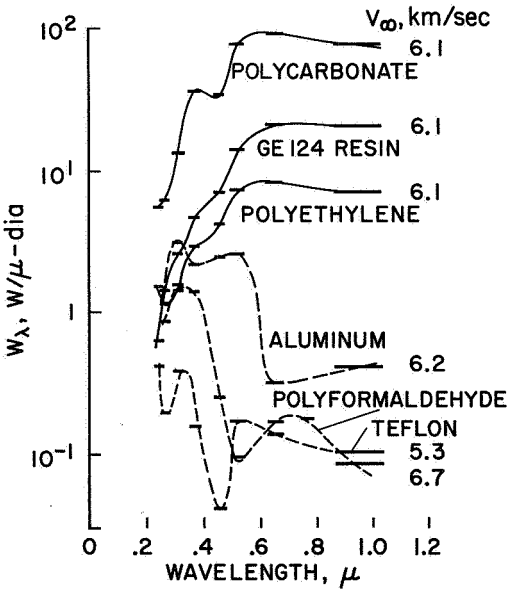

Figure 8.- Peak wake spectral radiation, $\rho_\infty/\rho_o = 0.08$.

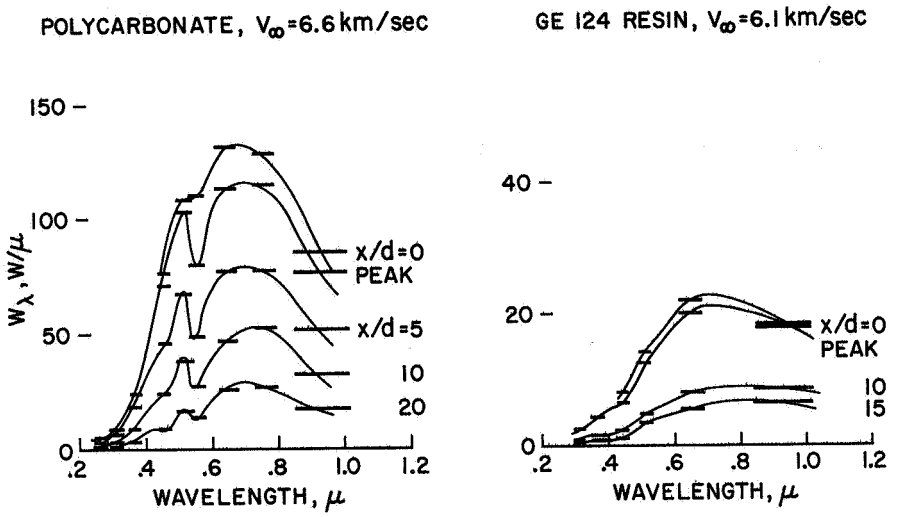

Figure 9.- Decay of wake radiance, ρ_∞/ρ_o = 0.08.

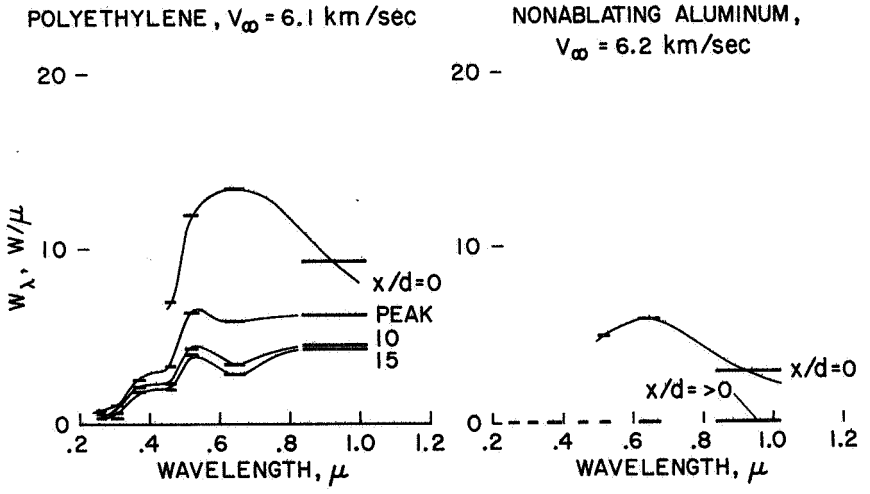

Figure 10.- Decay of wake radiance, ρ_∞/ρ_o = 0.08.

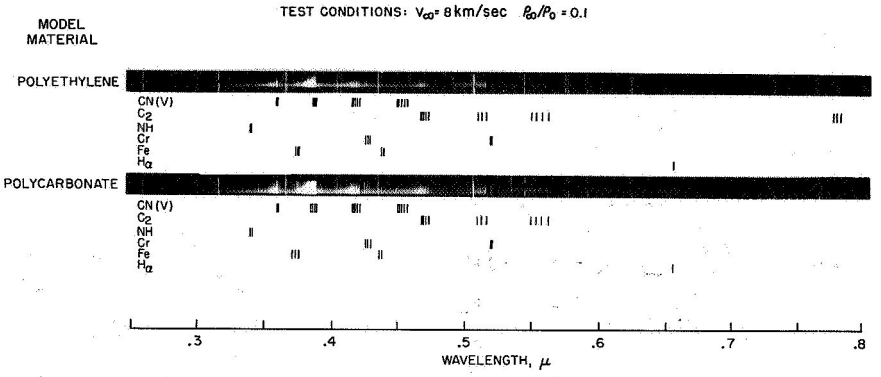

Figure 11.- Spectra of shock layer and near wake.

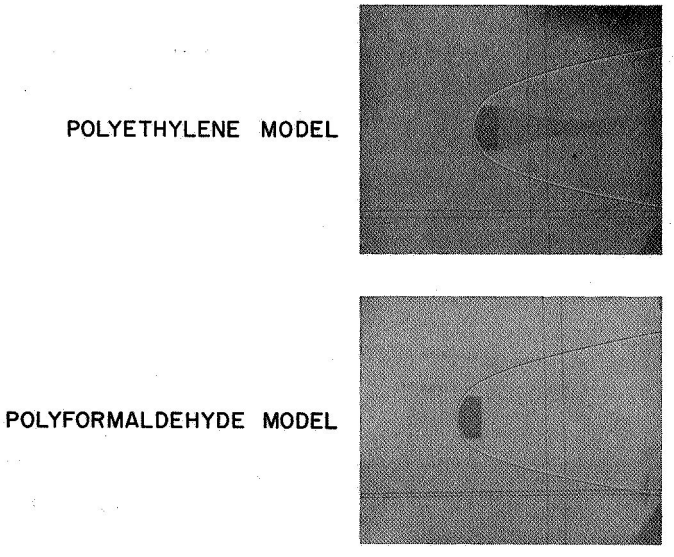

Figure 12.- Shadowgraphs of models in flight; $\rho_\infty/\rho_0 = 0.08$, $V_\infty = 6.3$ km/sec.

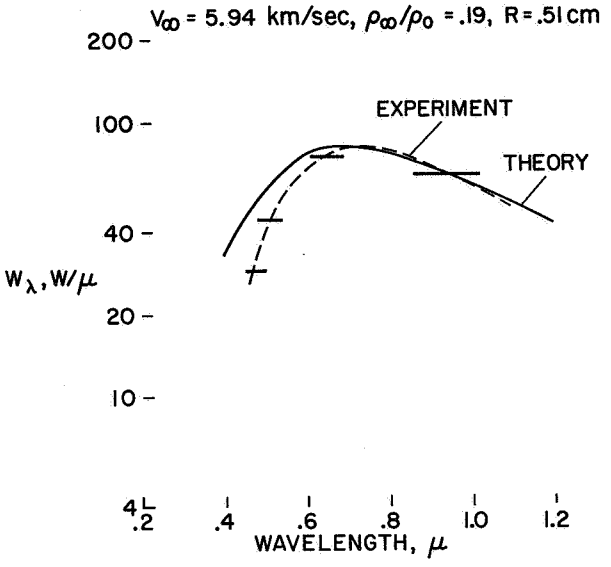

Figure 13.- Radiation from boundary layer of ablating polycarbonate model.

"The aeronautical and space activities of the United States shall be conducted so as to contribute . . . to the expansion of human knowledge of phenomena in the atmosphere and space. The Administration shall provide for the widest practicable and appropriate dissemination of information concerning its activities and the results thereof."

—NATIONAL AERONAUTICS AND SPACE ACT OF 1958

NASA SCIENTIFIC AND TECHNICAL PUBLICATIONS

TECHNICAL REPORTS: Scientific and technical information considered important, complete, and a lasting contribution to existing knowledge.

TECHNICAL NOTES: Information less broad in scope but nevertheless of importance as a contribution to existing knowledge.

TECHNICAL MEMORANDUMS: Information receiving limited distribution because of preliminary data, security classification, or other reasons.

CONTRACTOR REPORTS: Technical information generated in connection with a NASA contract or grant and released under NASA auspices.

TECHNICAL TRANSLATIONS: Information published in a foreign language considered to merit NASA distribution in English.

TECHNICAL REPRINTS: Information derived from NASA activities and initially published in the form of journal articles.

SPECIAL PUBLICATIONS: Information derived from or of value to NASA activities but not necessarily reporting the results of individual NASA-programmed scientific efforts. Publications include conference proceedings, monographs, data compilations, handbooks, sourcebooks, and special bibliographies.

Details on the availability of these publications may be obtained from:

SCIENTIFIC AND TECHNICAL INFORMATION DIVISION

NATIONAL AERONAUTICS AND SPACE ADMINISTRATION

Washington, D.C. 20546